2019 International Conference on Robotics and Automation (ICRA)
Palais des congres de Montreal, Montreal, Canada, May 20-24, 2019

Design and Experiments of a Squid-like Aquatic-aerial Vehicle with Soft Morphing Fins and Arms

Taogang Hou[1], Xingbang Yang[1,2,3,4,*], Haohong Su[1], Buhui Jiang[1], Lingkun Chen[1], Tianmiao Wang[1], Jianhong Liang[1]

***Abstract*— Aquatic-aerial multimodal vehicle is a new concept aircraft that can freely shuttle between water and air. Some of the natural organisms provide the inspiration to realize this multi-locomotion. Most of current prototypes use rigid link mechanisms or hinges to morph the structure thus to adapt to the aquatic-aerial environment, which is commonly complicated and bulky. In this paper, we present a novel prototype with pneumatically-driven soft fins and arms that can fold and spread just like the flying squid. The fins and arms can augment the lift force during flying by spreading and reduce drag force during swimming by folding. The performance of the morphable structures was investigated in wind and water tunnel. The results explain the tradeoff strategies of multimodal-locomotion between water and air, and verify the feasibility of the novel aquatic-aerial vehicle with soft morphable structures.**

I. INTRODUCTION

The aquatic-aerial vehicle has been widely focused on as a kind of aircraft with great potential applications. Some multi-locomotion vehicles launched from water into the air or plunge-diving from air into the water have been proposed [1]. Most of these robots are inspired by the natural aquatic-aerial amphibious organisms with the ability to fold and spread their wings or fins such as flying fish [2], [3], seabirds like gannet [4], [5], [6], [7], etc. This design allows the prototypes to quickly switch between water motion and aerial fly. However, these shape changeable prototypes are always realized by rigid link or hinges which connect to wings and fins, leading to a complicated structure and inconsistent with natural creatures, and making it hard to realize a perfect locomotion compared to its biological counterpart.

As shown in figure 1, flying squid is a very special one among all the amphibious organisms [8]. They can launch out of water by jet propulsion, followed with about 26.4-33.5m flying in the air and diving into the water [9]. In addition, the multi-locomotion of the natural flying squid can be separated into four steps: launching, jetting, gliding, and diving. The maximum speed can reach up to 11.2 m/s or 43.9-49.7 BL (body length)/s, while the limit state of ordinary fish is 25 BL/s [10]. Such amazing locomotion is greatly supported by the soft and flexible fins and arms of the squid except for the powerful water jet propulsion, and they roll down their fins around the body mantle and fold arms together to break the water surface during launching phase. When the speed of the squid reaching about 10 m/s [11], they will spread their fins and arms as wings to generate lift force and glide in the air. Thus the flying squid can flee from predators and quickly shuttle between water and air with the benefit of soft morphing fins and arms. The locomotion of the flying squid can be referred to a biomimetic prototype which can be used in pollution detection [12], maritime search [13] and rescue mission [14].

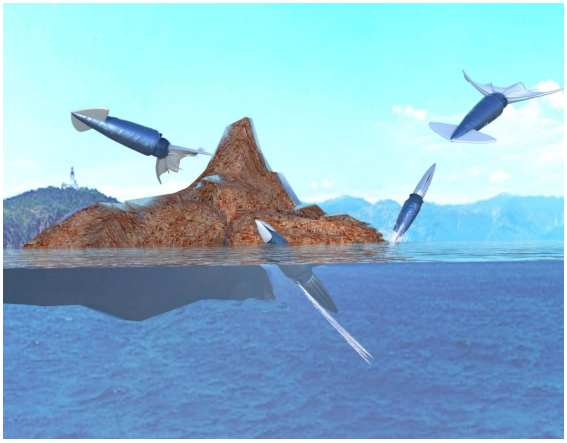

Fig. 1. Multi-locomotion of flying squid in launching, jetting, gliding and diving phases. Soft and flexible fins and arms can fold and spread in two fluids, to shuttle between water and air.

Inspired by the multi-locomotion of the flying squid, we first propose the concept of the application of soft morphing fins and arms on bionic prototype as shown in figure 2. The squid-like soft morphing fins and arms are made of flexible silicone and controlled by pneumatic actuator [15]. Unlike other multi-shape aquatic-aerial vehicles, the bionic soft fins and arms can roll and fold (shown in figure 2b) around the body rapidly just like the natural flying squid. It allows the vehicle to maintain a squid-like streamlined body when launching out from water and spread fins and arms to generate lift force when gliding in the air, making it possible to shuttle between water and air rapidly.

In this paper, we present a new type of squid-like aquatic-aerial vehicle with soft morphing fins and arms which can

Research was supported by the National Science Foundation of China grant numbers 61703023; Beijing Municipal Natural Science Foundation grant number 3184054; China Postdoctoral Science Foundation (2016M600892 and 2018T110024); China Scholarship Council (grant no. 201706025021).

[1] Taogang Hou is a Ph.D. Candidate in Mechanical Engineering and Automation & Shenyuan Honors College, Beihang University.

[1,2,3,4,*] Xingbang Yang is with School of Mechanical Engineering and Automation, School of Biological Science and Medical Engineering, Beijing Advanced Innovation Center for Biomedical Engineering at Beihang University and the MIT Media Lab at Massachusetts institute of technology. Correspondence: xingbang@mit.edu

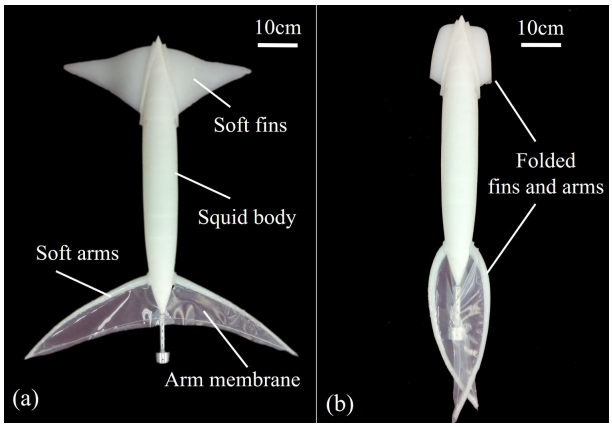

Fig. 2. Prototype of the squid-like aquatic-aerial vehicle with soft morphing structure. (a) Spread state. The soft fins and arms controlled by pneumatic actuators are spread in the jetting and gliding process. (b) Folded state. Fins roll around the mantle, and arms fold together in the launching and diving process.

fold and spread as the flying squid does. To further explore the tradeoff of the flying strategies of the natural squid, experiments of wind and water tunnel were conducted to investigate the performance of our prototype in spread (figure 2a) and folding (figure 2b) phases.

II. DESIGN

A. Objects

In order to improve the energy efficiency of movement, the body shape of the aquatic-aerial animals evolved to adapt to different liquid medium [16]. Most of the current aquatic-aerial multimodal vehicles refer to the living creatures with excellent aquatic-aerial amphibious characteristics in nature, most of which adopt the design of variable structures. However, these prototypes use traditional rigid structure that adds weight and complexity to the structure, and greatly reduces the biological relevance. Therefore, it is a key to improve the overall performance of aquatic-aerial multimodal vehicle by developing the variable structure with high bionic similarity and exploring the high-efficiency water-air transition mode.

In order to improve the performance of aquatic-aerial vehicle, we refer to the morphology of flying squids. We design a bionic prototype with soft variable structure fuselage. The fins and arms of the bionic prototype are made up of silica gel. There are soft actuators inside the fins and arms structure, which are driven pneumatically. By controlling the pneumatic device of the bionic prototype, the inflatable expansion and deflating shrinkage of the cavity are realized. This would enable the bionic prototype to fold or spread its soft fins and arms.

B. Theory

When the squid-like bionic prototype shuttle in the water, it will be subjected to lift force, gravity, buoyancy caused by fluid medium and drag force. We define an absolute coordinate system based on the Earth's fixed inertial system, as shown in figure 3, which is x, y, z. Set up a body coordinate system, and define its unit vectors x', y', z'. Considering that the values measured directly in wind tunnel and towing tank are axial forces and lateral forces in the body coordinate system, the lift force and drag force in the absolute coordinate system cannot be obtained directly from the experiment. Therefore, it is necessary to convert the values in the body coordinate system to the values in the absolute coordinate system. In addition, because of the symmetrical structure design of the squid-like bionic prototype, the lateral force is less when moving in the $x-y$ plane. Force in the z direction can be neglected for simplifying the calculation. Hence, the force transformation formula is shown as follows:

$$\begin{pmatrix} F_x \\ F_y \end{pmatrix} = \begin{pmatrix} cos\alpha & -sin\alpha \\ sin\alpha & cos\alpha \end{pmatrix} \begin{pmatrix} F'_x \\ F'_y \end{pmatrix} \tag{1}$$

where α is the attack angle, as shown in figure 5. In addition, lift coefficient and drag coefficient are important parameters to evaluate the flying performance of prototype. In order to verify the rationality of the variable structure design, this paper investigates the lift coefficient and drag coefficient in the wind tunnel. Lift coefficient C_L and drag coefficient C_D can be described as:

$$C_L = \frac{F_L}{\frac{1}{2}\rho_a v^2 s} \qquad C_D = \frac{F_D}{\frac{1}{2}\rho_a v^2 s} \tag{2}$$

where ρ_a represents the density of the air, s is the reference area, and v is the speed of the centroid of the prototype, which is expressed by the actual wind speed in the wind tunnel experiment.

Thrust of this pneumatic-driving prototype can be predicted by slug model [17]. Assuming that the orifice ejects fluids in a quiescent environment, the average jet velocity in the orifice area can be described by the mass transfer flow as [18], [19]:

$$U_j(t) = \frac{1}{\rho_w A}\dot{m} \tag{3}$$

where $\dot{m}$ is the instantaneous mass transfer in the orifice, A denotes the orifice area. And the instantaneous thrust $T(t)$ is presented as:

$$T(t) = U_j(t)\dot{m} = \frac{4}{\rho_w \pi D^2}\dot{m}^2 \tag{4}$$

where D is the diameter of the orifice. Assuming that t_e is the time required for jet expulsion, the average thrust equation is given by:

$$\overline{T} = \frac{1}{\rho_w A}\overline{\dot{m}} = \frac{4}{\rho_w \pi D^2}(\frac{m}{t_e})^2 \tag{5}$$

where m is the total water mass in the mantle cavity. Therefore, the average thrust is determined by the total mass of water m (0.6 kg), diameter of the orifice D (0.01m), and jet expulsion time t_e. In addition, the velocity of the prototype in air can be estimated by the momentum theorem.

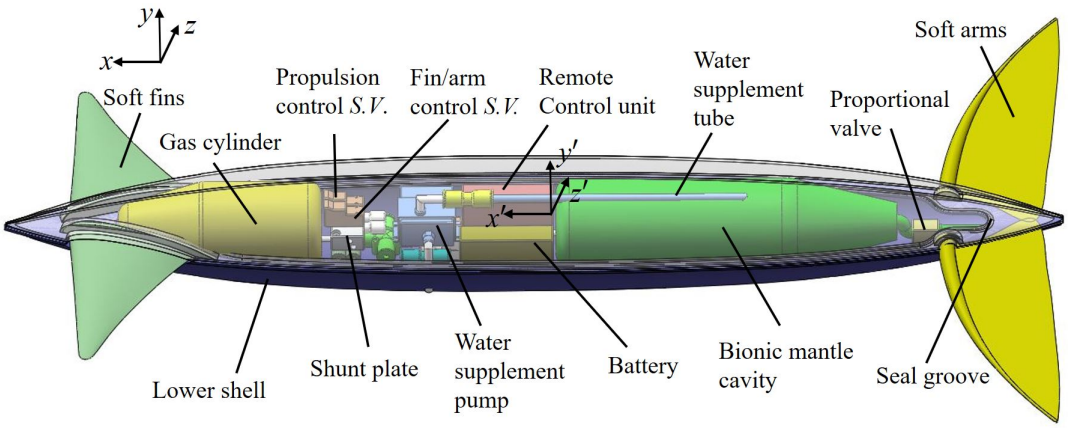

Fig. 3. The overall framework of squid-like prototype with the upper shell transparent. *S.V.* represents the solenoid valve controlled by the remote control unit. The gas cylinder provides compressed air and is connected to the bionic mantle cavity by the propulsion control *S.V.*. The jetting flow is adjusted by proportional valve.

C. Prototype

The soft morphing squid-like prototype, composed of body shell, pneumatic system, water supplement unit and electric control system, is shown in figure 3. The dimension parameters of the prototype are shown in table 1. The body shell is divided into upper and lower parts, and the space inside the body holds the control and power system. For a better performance, it is necessary to reduce the mass of the prototype as much as possible. In addition, to complete the multi-locomotion between water and air, the body shell must have enough mechanical strength that can withstand impact force. Therefore, the prototype is made of photosensitive resin material with low density and high strength, which is fabricated by 3D printer (SLA). A clamping slot, i.e., the seal groove, was designed between the upper and lower body shells, where the sealing ring is applied to ensure good waterproofness between the body space and the external environment.

The pneumatic system provides power to the jet propulsion and soft morphing actuator. The prototype adopts jet propulsion unit, which uses compressed gas in the gas cylinder to propel water jet from bionic mantle cavity by the control of the propulsion control *S.V.*. In addition, a silica gel membrane is used as the gas-liquid isolation layer in the bionic mantle cavity [20]. When the prototype was propelled by the jet flow, the gas from gas cylinder was pressed into the bionic mantle cavity to push the gas-liquid isolation layer moving backwards, and then the water on the other side was ejected from the jet orifice. After an injection cycle, a water supplement pump was adopted to suck water from external environment into mantle cavity. Like the flying squid in nature, the soft morphing squid-like prototype has three states: slow swimming underwater [21], trans-medium jet flight and air gliding. The first two states depend on a set of pneumatic system to control jet propulsion. Therefore, the jet orifice adopts the specially designed proportional valve to control the jet flow. When the valve is opened just a little bit, the injection water is less and the prototype moves slowly. On the contrary, when the valve is entirely opened, the injection water is fully propelled and the acceleration of the prototype reaches the maximum.

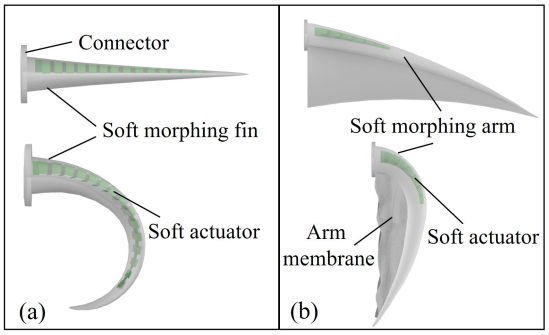

Fig. 4. Schematic of the soft morphing fins and arms, with transparency added to show the pneumatic soft actuator inside. (a) Soft fin in spread and folded phase. (b) Arm in spread and rolled state, with soft membrane forming a tail plane.

TABLE I
DIMENSION PARAMETERS OF THE SQUID-LIKE PROTOTYPE.

Fin and arm state	Total length(cm)	Fin span (cm)	Arm span (cm)	Maximum body diameter (cm)
Spread	78	48	60	13
Folded	78	15	16	13

The soft fin and arms made of silica gel, imitate the morphology features of the real flying squids fins and arms [22]. The outer surface and inner cavity of the fin and arm are formed by casting using 3D-printed mold. In order to generate greater lift force in the air, the soft fin was designed referring to Clark Y airfoil with large lift coefficient [23]. Inside the soft fins and arms, we designed some inflatable cavities, which were connected with gas cylinder by fin/arm control *S.V.* [24], [25]. After inflating gas, the soft fins and arms perform asymmetric deformation due to the cavity expansion, thus the spreading and folding deformation can be completed (shown in figure 4a). During folding, the soft

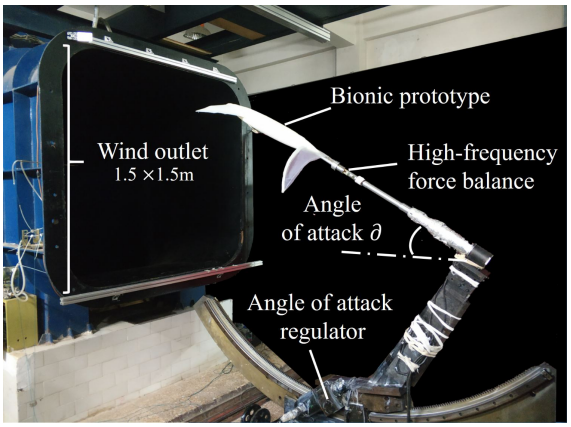

Fig. 5. Wind tunnel test apparatus. A worm drive regulator is used to adjust angle of attack α of the prototype. The bionic prototype is concentric with high frequency force balance in the tail. Size of the wind outlet is 1.5×1.5m, with turbulence degree of 0.08% which guarantees the ample quality flow field.

fins can be rolled around the body like the natural flying squid. Similar to the soft fins, the soft arms of the prototype can also be spread/folded by expansion/contraction of the inflatable cavity structure under positive/negative pressure (shown in figure 4b). With the cooperation of the soft fins, soft arms and pneumatic system, the soft morphing squid-like prototype can simulate the variable structure of the body of a real flying squid.

The gas cylinder refilling process is completed by an external air compressor through air supply channel on the lower shell. The jet orifice proportional valve (a ball valve) is connected to a metal steering gear through a connecting link. To determine the flow rate of jet propulsion, the metal steering gear can control the opening angle of the valve by turning the connecting link. In order to remotely control the prototype, a receiver is placed inside the body shell of the prototype with a radio frequency of 72 MHz. There is a micro-controller unit controlling the on-off of the relay and the metal steering gears motion angle as well as receiving and processing of the remote-control signal.

III. EXPERIMENTAL SETUP

A. Wind Tunnel

The wind tunnel experiment was conducted to investigate performance of the soft morphing squid-like prototype in the air (shown in figure 5). The prototype is placed in the flow field generated by the wind tunnel. A high-frequency force balance was attached to the tunnel floor, the data acquisition frequency of which is 1000 Hz. According to equation 5, jet expulsion time t_e can range from 0.3s to 1.5s by controlling proportional valve, so the average thrust can be estimated between 2.01N and 50.96 N accordingly. Furthermore, the weight of the prototype is 1.12kg. The velocity of the prototype in the air can be predicted between 2.73 m/s-13.64 m/s. Therefore, considering the minimum flow velocity of the wind tunnel is 5m/s, we set the speed of the wind tunnel flow from 5 m/s to 15 m/s, and the angle

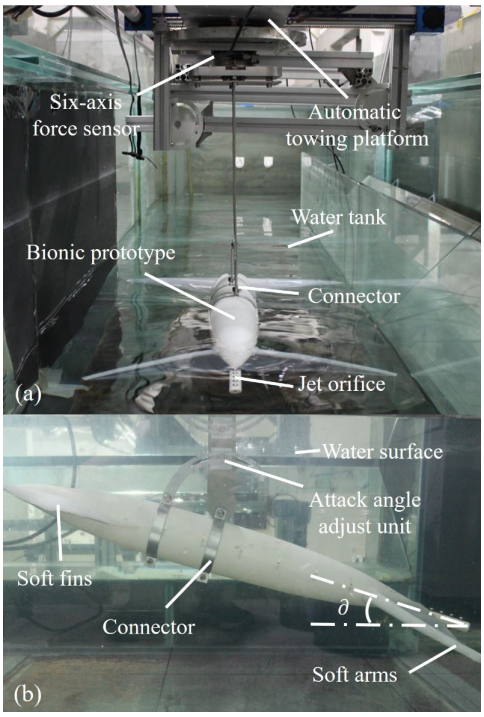

Fig. 6. Experimental setup of underwater towing test. (a) Overall view of the underwater towing system. The towing platform could move along the water tank in an accurate speed. The bionic prototype was connected to the six-axis force sensor mounted on the towing platform. (b) Lateral view of underwater configuration. An attack angle adjust unit was used to change the attack angle.

of attack α ranges from $-6°$ to $34°$. The prototype relied on the pneumatic system to spread and fold the soft fins and arms. In addition, a height-adjustable support screw was designed to adjust the angle of horizontal tail. The tail angle is selected as $0°$, $6°$, and $12°$.

B. Under water towing system

An underwater towing tank was used to test underwater hydrodynamic performance of the prototype. The movement of the prototype was towed by the towing platform (shown in figure 6a). A six-axis force sensor was used to record the three-axis force and the three-axis torque. An adjustment unit that can continuously adjust attack angle was designed to set more accurate attack angle α (shown in figure 6b). Like the wind tunnel experiment, the prototype was tested in spread and folded state of the soft fins and arms under different angles of attack. In order to simplify the experiment, the speed range of the experimental was set from 0.1 m/s to 0.6 m/s (maximum speed is limited by the towing tank system), and α is selected as $0°$ and $15°$.

IV. DISCUSSION

A. Results

In the wind tunnel experiment, we obtained the aerodynamic force of the prototype at different wind flow speeds and angles of attack. First, we obtained the drag force in the air when the soft fins and arms fold under different angles of attack and different speeds (shown in figure 7a). It can be

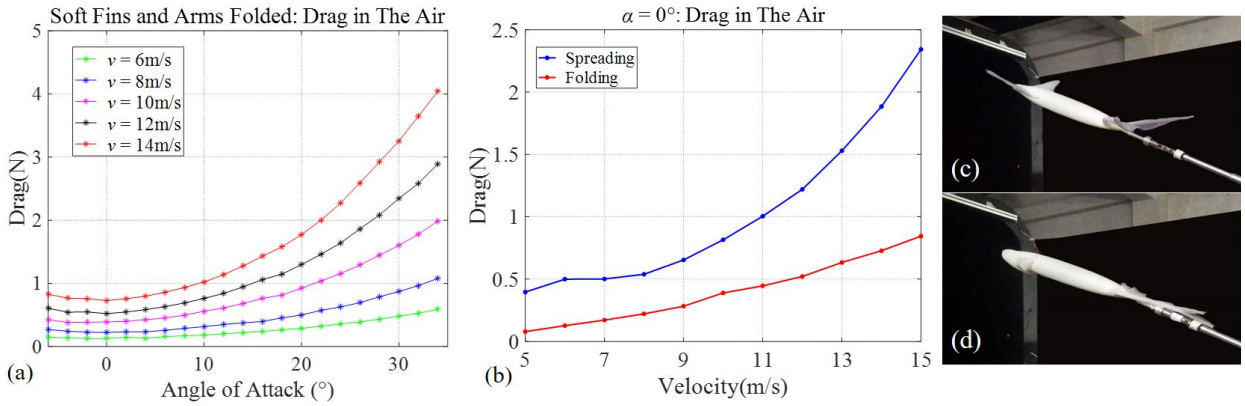

Fig. 7. Drag force of the prototype in the air phase. (a) The drag profiles when the angle of attack ranges from −6° to 34° in 2° increment, with soft fins and arms folded. Different colored lines represent different flow rates between 6m/s and 14m/s. (b) Comparison of the prototype drag in spread and folded state, under an angle of attack in 0°. (c) and (d) present flying posture in spread and folded state when the wind speed is 10m/s respectively.

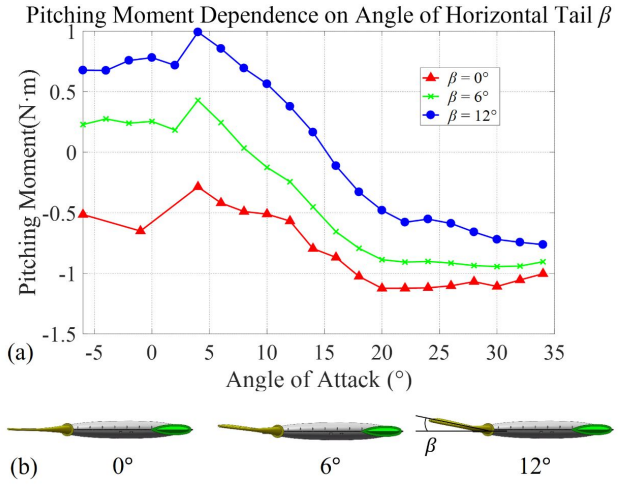

Fig. 8. The effect of horizontal tail angle on pitch moment. (a) Pitch moment of the squid-like prototype under different tail angles when changing angle of attack. (b) Prototype in different horizontal tail angles 0°, 6° and 12°.

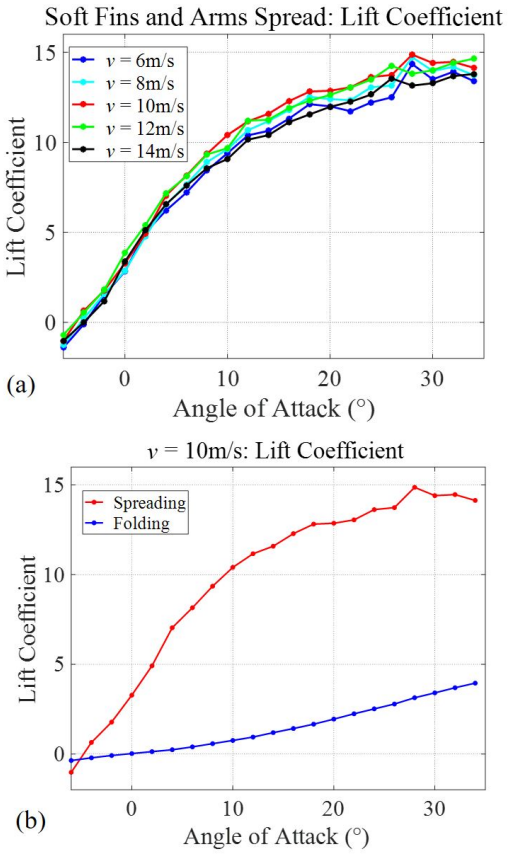

Fig. 9. (a) Lift coefficient curves of the spread state at 6, 8, 10, 12 and 14 m/s. (b) Lift coefficient curves for the spread state compared with folded state under 10 m/s wind flow speed.

seen that when the $\alpha = 0°$, the prototype is subjected to the smallest drag force. With the angle of attack increasing, the drag force of the prototype increases simultaneously.

In addition, we also compare the drag force of the prototype between the spread and folded states of soft fins and arms when α = 0°. As shown in figure 7b, it can be known that the prototype is subjected to a higher drag when the soft fins and arms are spreading. This result explains why the natural flying squid still keeps folding the fins and arms during the acceleration process after launching out of water. The prototype has a better acceleration performance in the air when $\alpha = 0°$ and the soft fins and arms are in folded state.

As shown in figure 8, with the angle of attack increasing, the pitching moment of the prototype first increases and then decreases. When $\alpha = 4°$, the pitching moment of the prototype reaches the maximum value, and then tends to be stable after 20°. As β increases, the pitching moment of the prototype also increases, indicating that the squid could control the flying attitude through changing the horizontal tail angle.

This study also focuses on the lift force provided by the aerodynamic shape at different angles of attack when the soft fins and arms spread. The results indicate that as the angle of attack increases, the lift coefficient of the prototype increases accordingly, and then tends to be convergent (shown in figure 9a). When $\alpha = 28°$, the lift coefficient can achieve

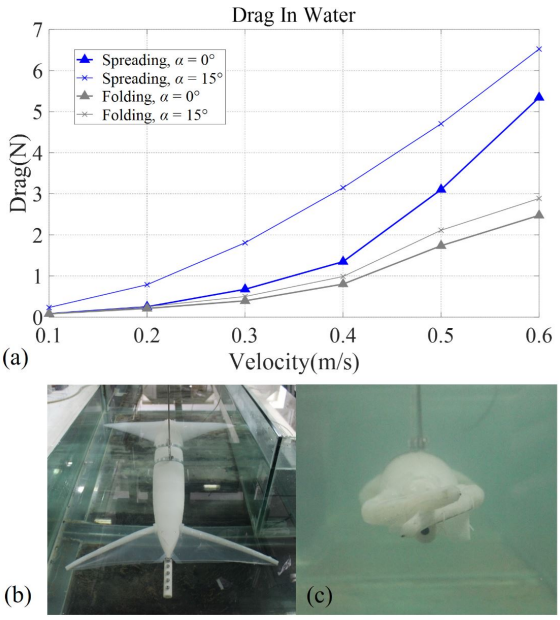

Fig. 10. Drag of the prototype under water. (a) Drag of the prototype in spread and folded state underwater when $\alpha = 0°$ and $\alpha = 15°$, with a towing velocity between 0.1 m/s and 0.6 m/s in 0.1 increment. (b) Fins and arms are spread. (c) Fins roll around the body and arms folded together.

a maximum value. As shown in figure 9b, the prototype in spread state is able to generate a significantly higher lift coefficient than folded state, which helps a long way gliding in the air.

In the underwater towing test, the drag force of the prototype under different conditions is obtained. When the soft fins and arms are spreading, the area of the prototype contacting with the aqueous medium increases, and the drag force is also increased (shown in figure 10). In addition, when the soft fins and arms are spreading or folding, the drag force increases with the angle of attack.

B. Variable Structure Design

These experiments have demonstrated the benefit of the variable structure design of the soft morphing squid-like prototype. When the prototype folds its fins and arms and accelerate under water, its spindle shape can well reduce the drag force. In addition, when the prototype is jetting out of water in the accelerated phase, the drag force is much greater as the attack angle increases. Therefore, selecting a suitable angle of attack with low drag force is beneficial to the launching acceleration. Moreover, the lift force of the prototype with soft fins and arms in spread state is much larger than folded state (e.g., the lift forces in folded and spread states are 3.2 N and 15.1 N, respectively, when $\alpha = 30°$ and $v = 14$ m/s), so the prototype should spread fins and arms in the gliding phase.

Through the pneumatic system, the prototype could be propelled by the jet propulsion as shown in figure 11, and the soft morphing fins and arms were controlled to spread and fold to realize the switching between different aerodynamic shapes. It is adaptive to different mediums and different

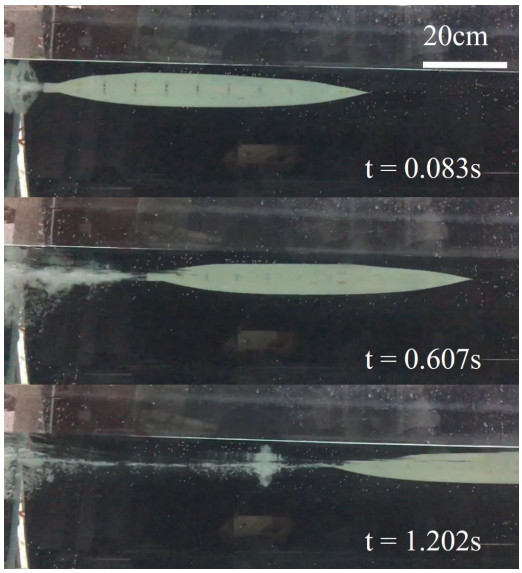

Fig. 11. Image of the squid-like prototype being propelled by water jet flow underwater.

locomotion stages. The unique inflatable cavity design allows the soft fins and arms to spread and fold as expected, and makes the prototype to have a good biological morphology.

V. CONCLUSIONS

In this paper, we propose the new concept of soft morphing structure for aquatic-aerial vehicle, and make a jet propelled squid-like prototype. The soft pneumatic morphing design makes it possible for the prototype to execute quick shuttle between water and air.

The soft fins and arms driven by soft actuator can fold and spread without the help of any outer links and hinges, which guarantees a streamlined appearance in folded or spread state, and reduces redundancy structure.

The presented soft morphing squid-like prototype has also been tested in wind tunnel and underwater towing tank. The results show that the morphing design greatly helps the prototype multi-locomotion, and reveal the superiority of the natural flying squid movement.

In conclusion, this research greatly improved the similarity between the bionic prototype and its biological counterpart. Wind tunnel and underwater experiments helped to explore the tradeoff between different multi-locomotion strategies. The complete prototype will provide new ideas for the study of aquatic-aerial vehicles.

ACKNOWLEDGMENT

We wish to thank Education Ministry Key Laboratory for Fluid Dynamics for providing wind tunnel of experiment. Wenguang Sun and Qihang Yuan aided the experiment setup. Siyang Zhang contributed to editing the manuscript. Thank Yang Liu's help in improving the English language.

REFERENCES

[1] X. B. Yang, T. M. Wang, J. H. Liang, G. C. Yao, and M. Liu, "Survey on the novel hybrid aquatic-aerial amphibious aircraft: aquatic unmanned aerial vehicle (AquaUAV)," *Progress in Aerospace Sciences*, vol. 74, pp. 131-151, 2015.

[2] A. Gao and A. H. Techet, "Design considerations for a robotic flying fish," *OCEANS'11 MTS/IEEE KONA*, pp. 1-8, 2011.

[3] J. S. Izraelevitz and M. S. Triantafyllou, "A Novel Degree of Freedom in Flapping Wings Shows Promise for a Dual Aerial/Aquatic Vehicle Propulsor," *IEEE International Conference on Robotics and Automation (ICRA)*,pp. 5830-5837, 2015.

[4] R. Siddall and M. Kovac, "A water jet thruster for an aquatic micro air vehicle," *IEEE International Conference on Robotics and Automation (ICRA)*, pp. 3979-3985, 2015.

[5] A. Fabian, Y. F. Feng, and E. Swartz, "Hybrid aerial underwater vehicle," *Lexington : MIT Lincoln Lab*, SCOPE Projects, 2012.

[6] T. M. Wang, X. B. Yang, J. H. Liang, G. C. Yao, and W. D. Zhao, "CFD based investigation on the impact acceleration when a gannet impacts with water during plunge diving," *Bioinspiration & biomimetics*, vol. 8, no. 3, p. 036006, 2013.

[7] D. A. Shealer, "Foraging behavior and food of seabirds," *Biology of marine birds*, CRC press, pp. 150-191, 2001.

[8] R. O'Dor, J. Stewart, W. Gilly, J. Payne, T. C. Borges, and T. Thys, "Squid rocket science: how squid launch into air," *Deep Sea Research Part II: Topical Studies in Oceanography*, vol. 95, pp. 113-118, 2013.

[9] K. Muramatsu, J. Yamamoto, and T. Abe, "Oceanic squid do fly," *Marine biology*, vol. 160, no. 5, pp. 1171-1175, 2013.

[10] C. S. Wardle, "Limit of fish swimming speed," *Nature*, 255.5511, 725, 1975.

[11] R. O'Dor and S. N. Mendon, "Analysis of Sthenoteuthis oualaniensis flying behaviour from recorded video," *Cephalopod International Advisory Council Conference*, vol. 122, p. 13, 2015.

[12] R. Siddall and M. Kovac, "Launching the aquamav: bioinspired design for aerialaquatic robotic platforms," *Bioinspiration & biomimetics*, vol. 9, no. 3, p. 031001, 2014.

[13] R. R Murphy, E. Steimle, and C. Griffin, "Cooperative use of unmanned sea surface and micro aerial vehicles at Hurricane Wilma," *Journal of Field Robotics*, vol. 25, no. 3, pp. 164-180, 2008.

[14] S. Kawatsuma, M. Fukushima, and T. Okada, "Emergency response by robots to fukushima-daiichi accident: summary and lessons learned," *Industrial Robot: An International Journal*, vol. 39, no. 5, pp. 428-435, 2012.

[15] B. Mosaswgh, P. Polygerinos, and C. Keplinger, "Pneumatic networks for soft robotics that actuate rapidly," *Advanced Functional Materials*, vol. 24, no. 15, p. 2109, 2014.

[16] J. Davenport, "How and why do flying fish fly?" *Reviews in Fish Biology and Fisheries*, vol. 4, no. 2, pp. 184-214, 1994.

[17] K. Mohseni, H. Ran, and T. Colonius, "Numerical experiments on vortex ring formation," *Journal of Fluid Mechanics*, vol. 430, pp. 267282, 2001.

[18] M.Krieg and K. Mohseni, "Thrust characterization of a bioinspired vortex ring thruster for locomotion of underwater robots," *IEEE Journal of Oceanic Engineering*, vol. 33, no. 2, pp. 123-132, 2008.

[19] R. Siddall and M. Kovac, "Fast aquatic escape with a jet thruster," *IEEE/ASME Transactions on Mechatronics*, vol. 22, no. 1, pp. 217-226, 2017.

[20] F. Giorgio-Serchi, A. K. Lidtke, and G. D. Weymouth, "A soft aquatic actuator for unsteady peak power amplification," *IEEE/ASME Transactions on Mechatronics*, vol. 23, no. 6, pp. 2968-2973, 2018.

[21] E. J. Anderson and M. E. DeMont, "The mechanics of locomotion in the squid Loligo pealei: locomotory function and unsteady hydrodynamics of the jet and intramantle pressure," *Journal of Experimental Biology*, vol. 203, no. 18 , pp. 2851-2863, 2000.

[22] P. Polygerinos, Z.Wang, J. T. Overvelde, K. C. Galloway, R. J. Wood, K. Bertoldi, and C. J. Walsh, "Modeling of soft fiber-reinforced bending actuators," *IEEE Transactions on Robotics*, vol. 31, no. 3, pp. 778-789, 2015.

[23] A. Piccirillo, "The Clark Y Airfoil - A historical retrospective," *World Aviation Conference*, 2000.

[24] K. Suzumori, "Flexible microactuator: 1st report, static characteristics of 3 DOF actuator," *Transactions of the Japan Society of Mechanical Engineers*, vol. 55, no. 518, pp. 2547-2552, 1989.

[25] D. Rus and M. T. Tolley, "Design, fabrication and control of soft robots," *Nature*, vol. 521, no. 7553, p. 467, 2015.